Journal of Neurochemistry, 2003, **87**, 676–685 doi:10.1046/j.1471-4159.2003.02058.x

Polarized actin bundles formed by human fascin-1: their sliding and disassembly on myosin II and myosin V *in vitro*

Ryoki Ishikawa,* Takeshi Sakamoto,† Toshio Ando,† Sugie Higashi-Fujime‡ and Kazuhiro Kohama*

**Department of Pharmacology, Gunma University School of Medicine, Maebashi, Gunma*

†Department of Physics, Faculty of Science, Kanazawa University, Ishikawa

‡Department of Molecular Biology, Faculty of Science, Nagoya University, Aichi, Japan

Abstract

Fascin-1 is a putative bundling factor of actin filaments in the filopodia of neuronal growth cones. Here, we examined the structure of the actin bundle formed by human fascin-1 (actin/fascin bundle), and its mode of interaction with myosin *in vitro*. The distance between cross-linked filaments in the actin/bundle was 8–9 nm, and the bundle showed the transverse periodicity of 36 nm perpendicular to the bundle axis, which was confirmed by electron microscopy. Decoration of the actin/fascin bundle with heavy meromyosin revealed that the arrowheads of filaments in the bundle pointed in the same direction, indicating that the bundle has polarity. This result suggested that fascin-1 plays an essential role in polarity of actin bundles in filopodia. In the *in vitro* motility assay, actin/fascin bundles slid as fast as single actin filaments on myosin II and myosin V. When myosin was attached to the surface at high density, the actin/fascin bundle disassembled to single filaments at the pointed end of the bundle during sliding. These results suggest that myosins may drive filopodial actin bundles backward by interacting with actin filaments on the surface, and may induce disassembly of the bundle at the basal region of filopodia.

Keywords: filopodium, growth cone, retrograde flow.

J. Neurochem. (2003) **87,** 676–685.

Growth cones of developing nerve cells extend filopodia from their leading edge, the dynamics of which are implicated in the elongation and path finding of axons (Bentley and Toroian-Raymond 1986; Chien *et al.* 1993). Generation of filopodia is closely related to the growth direction of axons. Local Ca^{2+} influx into the *Xenopus* growth cone by application of a neurotransmitter with a micropipette induces generation of filopodia, resulting in the turning of growth cone toward the pipette (Zheng *et al.* 1994). When Ca^{2+} concentration is elevated in a local area of grasshopper growth cone, the number and length of filopodia in that area increase (Lau *et al.* 1999). Moreover, continuous elevation of Ca^{2+} concentration in the right half causes the *Xenopus* growth cone to turn to the right (Zheng 2000). Netrin, an attractive guidance molecule of axons, induces elevation of Ca^{2+} concentration in growth cones, resulting in generation of filopodia and turning of the growth cone toward the netrin-gradient (Hong *et al.* 2000). These reports support the idea that generation of filopodia determines the direction of axonal growth.

A typical filopodium is composed of a bundle of 15–20 actin filaments (F-actin), which are tightly packed with a distance of 7–8 nm between cross-linked filaments (Lewis and Bridgman 1992; Steketee *et al.* 2001; Steketee and Tosney 2002; Svitkina *et al.* 2003). The barbed end of F-actin in a bundle faces the filopodial tip (Lewis and Bridgman 1992). Observation of actin dynamics in filopodia reveals that (i) actin is incorporated into the tips of filopodia (Okabe and Hirokawa 1991), (ii) actin bundles of filopodia continuously move from the tips toward the basal region; this is known as 'retrograde flow' (Okabe and Hirokawa 1991; Lin *et al.* 1996; Mallavarapu and Mitchison 1999) and (iii) in the basal region, actin bundles disassemble to F-actin and/or depolymerize to globular actin (G-actin) (Katoh *et al.* 1999; Mallavarapu and Mitchison 1999).

Received April 18, 2003; revised manuscript received July 7, 2003; accepted July 17, 2003.

Address correspondence and reprint requests to Dr Ryoki Ishikawa, Department of Pharmacology, Gunma University School of Medicine, Maebashi, Gunma 371–8511, Japan.

E-mail: ryoki1@med.gunma-u.ac.jp

Abbreviations used: AFM, atomic force microscopy; F-actin, filamentous actin; G-actin, globular actin; HMM, heavy meromyosin; MLCK, myosin light chain kinase.

In neurons, an actin-bundling protein fascin co-localizes with actin bundles in the filopodia of growth cones (Edwards and Bryan 1995; Sasaki *et al.* 1996; Cohan *et al.* 2001). Suppression of fascin expression by antisense oligonucleotide causes loss of filopodia (Edwards and Bryan 1995), suggesting that fascin is an actin-bundling factor of filopodia in neurons. Fascins belong to a unique family of actin-bundling proteins, including sea urchin fascin (Kane 1975; Otto *et al.* 1979; Bryan *et al.* 1993), HeLa cell 55-kDa actin-bundling protein (Yamashiro-Matsumura and Matsumura 1985; Ishikawa *et al.* 1998), and the gene products of *Drosophila* singed (Cant *et al.* 1994; Tilney *et al.* 1995). Recently, fascins have been classified into three groups by their amino acid sequences, fascin-1 (ubiquitous type), fascin-2 (retinal type), and fascin-3 (testis type) (Kureishy *et al.* 2002). Fascin-1 localizes in dynamic actin structures such as filopodia and microspikes in a variety of cell types (for review, Otto 1994; Edwards and Bryan 1995; Kureishy *et al.* 2002). The molecular structure of actin bundles formed by fascin-1 (designated as 'actin/fascin bundles' in this paper) is well documented. Electron micrographs of the crude actin bundles from sea urchin eggs show transverse periodicity of 11 nm (Bryan and Kane 1978; DeRosier and Censullo 1981). Optical diffraction studies predict that F-actin in bundles will be hexagonally packed with polarity (DeRosier and Censullo 1981). However, reconstituted actin/fascin bundles from mouse show 36-nm periodicity with an angle of 60° to the bundle axis (Edwards *et al.* 1995), but polarity of bundles has not yet been examined.

In this report, we present direct evidence that the actin/fascin bundle from human source has polarity. In the *in vitro* motility assay, actin/fascin bundles slide as fast as single F-actin filaments on myosin II and myosin V. On the surface coated with myosin at a high density, the bundles disassemble into individual F-actin filaments from the pointed end during their sliding. Based on these results, we discuss a possible mechanism of structural dynamics in the filopodia of nerve growth cones.

Materials and methods

Reagents and proteins

ATP was purchased from Roche (Basel, Switzerland), and the rest of the chemicals were purchased from Sigma (St Louis, MO, USA). Human fascin-1 was expressed in bacteria and purified as described (Ono *et al.* 1997). Non-muscle myosin II was purified from porcine brain by the method of Pato *et al.* (1996). Skeletal muscle myosin II was purified from rabbit as described (Perry 1955). Myosin V was purified from the brain of newly hatched chicken by the method of Cheney (1998) with slight modification (Sakamoto *et al.* 2000). Myosin light chain kinase was purified from chicken gizzard (Adelstein and Klee 1981), and actin was purified from chicken breast muscle (Matsumura *et al.* 1982). Purified proteins were checked by sodium dodecyl sulfate – polyacrylamide gel electrophoresis (SDS–PAGE).

Electron microscopy

G-actin or F-actin (12 μM) was mixed with 3.6 μM fascin-1 in buffer A [100 mM KsCl and 25 mM HEPES (pH 7.6)] at room temperature (20–25°C) for 1 h. The solutions were diluted 10 times with buffer A and mounted on a grid. After washing with a few drops of buffer, bundles were negatively stained with 1% uranyl acetate. For heavy meromyosin (HMM) decoration, bundles on the grid were treated with 0.21 μM HMM in buffer A for 1 min, washed with several drops of buffer A, and stained with 1% uranyl acetate. Samples were observed with a JEM1010 microscope (JOEL, Tokyo, Japan) operating at 80 kV.

Atomic force microscopy

F-actin (2 μM) was mixed with 0.2 μM fascin-1 in 25 mM KCl, 2 mM $MgCl_2$, 0.2 mM $CaCl_2$, 0.1 mM NaN_3, and 25 mM imidazole-HCl (pH 7.6) for 30 min on ice, and a drop of the mixture was placed on mica pre-coated with poly L-lysine. After incubation for 3 min, the sample was rinsed with the same buffer, and imaged with atomic force microscopy (AFM), as described previously (Ando *et al.* 2001).

In vitro motility assay

Skeletal muscle myosin II in the filamentous form was absorbed on the nitrocellulose-coated glass surface of the assay chamber in 25 mM KCl and 20 mM Tris-Cl (pH 7.6). Skeletal muscle myosin II in the monomeric form was absorbed in 600 mM KCl and 20 mM Tris-Cl (pH 7.6). F-actin (5.8 μM) labelled with rhodamine-phalloidin was bundled with fascin-1 (2.0 μM) in 100 mM KCl and 20 mM Tris-Cl (pH 7.6) overnight on ice. Solutions were diluted to 1/100 with buffer A containing 25 mM KCl, 2 mM $MgCl_2$, and 25 mM imidazole-Cl (pH 7.0), then applied to the assay chamber. In an experiment to measure brightness of filaments, 2 nM F-actin labelled with rhodamie-phalloidin was added to the assay solution just before observation. Motility was assayed as previously described (Toyoshima *et al.* 1987) in buffer B, which contained 25 mM KCl, 2 mM $MgCl_2$, 2 mM ATP, 100 mM 2-mercaptoethanol, 0.216 mg/mL glucose oxidase, 0.036 mg/mL catalase, 4.5 mg/mL glucose, and 25 mM imidazole-Cl (pH 7.0). Motility on non-muscle myosin II was assayed as described (Pato *et al.* 1996). Non-muscle myosin II (0.12–0.24 μM) was absorbed on the nitrocellulose-coated glass surface in 500 mM NaCl, 0.1 mM EGTA, 10 mM DTT, and 10 mM MOPS (pH 7.3), and was phosphorylated by mounting 0.10 μM myosin light chain kinase (MLCK) and 0.2 μM calmodulin in 20 mM KCl, 5 mM $MgCl_2$, 1 mM ATP, 0.1 mM EGTA, 0.2 mM $CaCl_2$, 5 mM DTT, and 20 mM MOPS (pH 7.2) for 2 min at room temperature. After wash out with MLCK and calmodulin, motility of actin/fascin bundles were assayed in 80 mM KCl, 5 mM $MgCl_2$, 2 mM ATP, 0.1 mM EGTA, 100 mM 2-mercaptoethanol, 0.216 mg/mL glucose oxidase, 0.036 mg/mL catalase, 4.5 mg/mL glucose, and 20 mM MOPS (pH 7.2). Motility on myosin V was assayed with buffer B, except that KCl concentration was 75 mM and 1 mM EGTA was added. The movement of F-actin or actin/fascin bundles was monitored under a fluorescence microscope (Axioplan, Zeiss, Oberkochen, Germany) equipped with a SIT camera (C2400; Hamamatsu Photonics, Hamamatsu, Japan). Images were saved in videotape, transferred to a personal computer, and processed with NIH image software. Absolute angle change of the

track of a moving bundle was measured at intervals of 0.25 s for 4 s, and the values obtained for 4 s were averaged and defined as a momentary angle change of each bundle.

ATPase activity

Skeletal muscle myosin II (0.10 μM) was mixed with actin/fascin bundle (4.2 μM actin and 2.2 μM fascin) or F-actin (4.2 μM) in 2 mM ATP, 2 mM $MgCl_2$, 100 mM KCl, 20 mM Tris-Cl (pH 7.6) at 25°C for 5 min. The amount of Pi liberated was determined by the malachite green method of Kodama *et al.* (1986).

Results

Polarity of actin bundles formed by human fascin-1

Actin/fascin bundles were observed by electron microscopy (Figs 1a and b) and AFM (Fig. 1c). The bundles showed transverse periodicity of 36 nm perpendicular to the bundle axis (arrowheads). A typical bundle contained 14–16 F-actin filaments, which were tightly packed, with a distance of 8.7–9.0 nm between cross-linked filaments (Table 1). Width and length of actin/fascin bundles were 120–140 nm and 5–8 μm, respectively (Table 1). These values were quite comparable with those of an actin bundle in filopodia (Lewis and Bridgman 1992; Steketee *et al.* 2001; Svitkina *et al.* 2003). However, (Tseng *et al.* 2001) reported the side-branching of the bundle *in vitro*, but we failed to observe side-branching of the bundle under our assay conditions.

To elucidate the orientation of F-actin in actin/fascin bundles, we decorated F-actin with skeletal muscle HMM (Fig. 2). When actin/fascin bundles were formed from F-actin, HMM failed to penetrate inside the bundles, and only decorated filaments in the bundle surface (data not shown). Therefore, G-actin was polymerized in the presence of fascin, and then the bundle was decorated with HMM (Fig. 2a). 'Arrowhead structures' of the filaments in the bundle pointed in the same direction (Fig. 2a, arrowheads), although we failed to detect 'arrowhead structures' in some filaments (Fig. 2a, asterisks). When the bundles were decorated with HMM just after mixing F-actin with fascin-1, the same results regarding polarity of the bundle were obtained (Fig. 2b). These results were confirmed by quantifying the orientation of F-actin in the bundles (Table 2). Thus, we concluded that actin/fascin bundles formed *in vitro* had polarity, as is observed in actin bundles of filopodia.

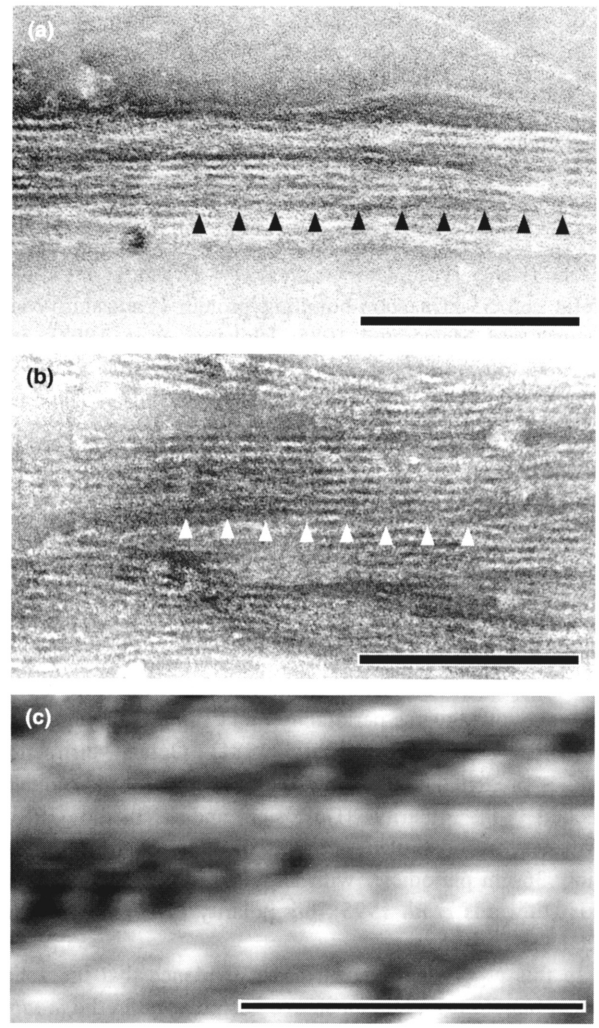

Fig. 1 Periodic structure of actin/fascin bundles. Electron micrographs of a negatively stained bundle (a and b), and atomic force micrograph (c). (a) Bundles were formed by mixing G-actin with fascin-1 in the presence of 100 mM KCl, then stained with 1% uranyl acetate. (b) Bundles were formed by mixing F-actin with fascin-1, and stained with 1% uranyl acetate. (c) Actin/fascin bundles were placed on mica pre-coated with poly L-lysine. A 500 × 500 nm area was imaged by AFM with 200 × 200 pixels. Note the periodicity of 36 nm in the bundles (arrowheads in a and b). Bars, 200 nm.

Sliding of actin/fascin bundles on skeletal muscle myosin II

We examined whether actin/fascin bundles could slide on the surface coated with skeletal muscle myosin II in the *in vitro* motility assay (Fig. 3). Actin/fascin bundles labelled with rhodamine-phalloidin appeared like 'needles' at low sensitivity of the camera (arrow in Fig. 3a, time 0 s), and like 'fireballs' at a sensitivity at which single F-actin filaments were observable (arrowhead in Fig. 3b, time 0 s). These actin/fascin bundles moved on myosin II (Figs 3a and b). Trajectory of an individual actin/fascin bundle revealed that the actin/fascin bundle moved with little change in direction (Fig. 3d), while single F-actin filaments frequently changed their directions (Fig. 3e). Averaged momentary angle changes of actin/fascin bundles and single F-actin filaments were 14 ± 4.5 degree/s and 41.8 ± 23.7 degree/s (mean ± SD, $n = 25$), respectively (see Materials and methods). Because actin/fascin bundles were straight (Fig. 3a) and compact

Table 1 Size of actin/fascin bundle

Fascin/actin ratio (actin; 12 μM)	Number of filaments[a] in the bundle	Width[a] (nm; m ± SD)	Distance between cross-linked filaments (nm; m ± SD)	Length[b] (μm; m ± SD)	Dilute to *in vitro* motility assay condition[c]
1 : 3[d]	15.0 + 4.7 ($n = 14$)	136 ± 44 ($n = 14$)	9.0 ± 0.9 ($n = 14$)	5.4 ± 2.4 ($n = 50$)	Keep bundle
1 : 3[e]	16.0 ± 9.3 ($n = 21$)	141 ± 82 ($n = 21$)	8.9 ± 1.1 ($n = 21$)	6.3 ± 2.9 ($n = 50$)	Keep bundle
1 : 5[d]	13.6 ± 4.3 ($n = 9$)	116 ± 35 ($n = 9$)	8.7 ± 0.9 ($n = 9$)	6.4 ± 2.2 ($n = 50$)	Keep bundle
1 : 10[d]	Not examined	Not examined	Not examined	7.7 ± 3.0 ($n = 50$)	Disassemble to F-actin

[a]Measured from EM pictures. [b]Rhodamine-phalloidin labelled bundes were diluted 10 times, and observed with a fluorescence microscope. [c]Rhodamine-phalloidin labelled-bundles were diluted to a final concentration of F-actin of 0.058 μM, and observed 30 min after dilution. [d]F-actin was mixed with fascin-1. [e]G-actin was polymerized in the presence of fascin-1.

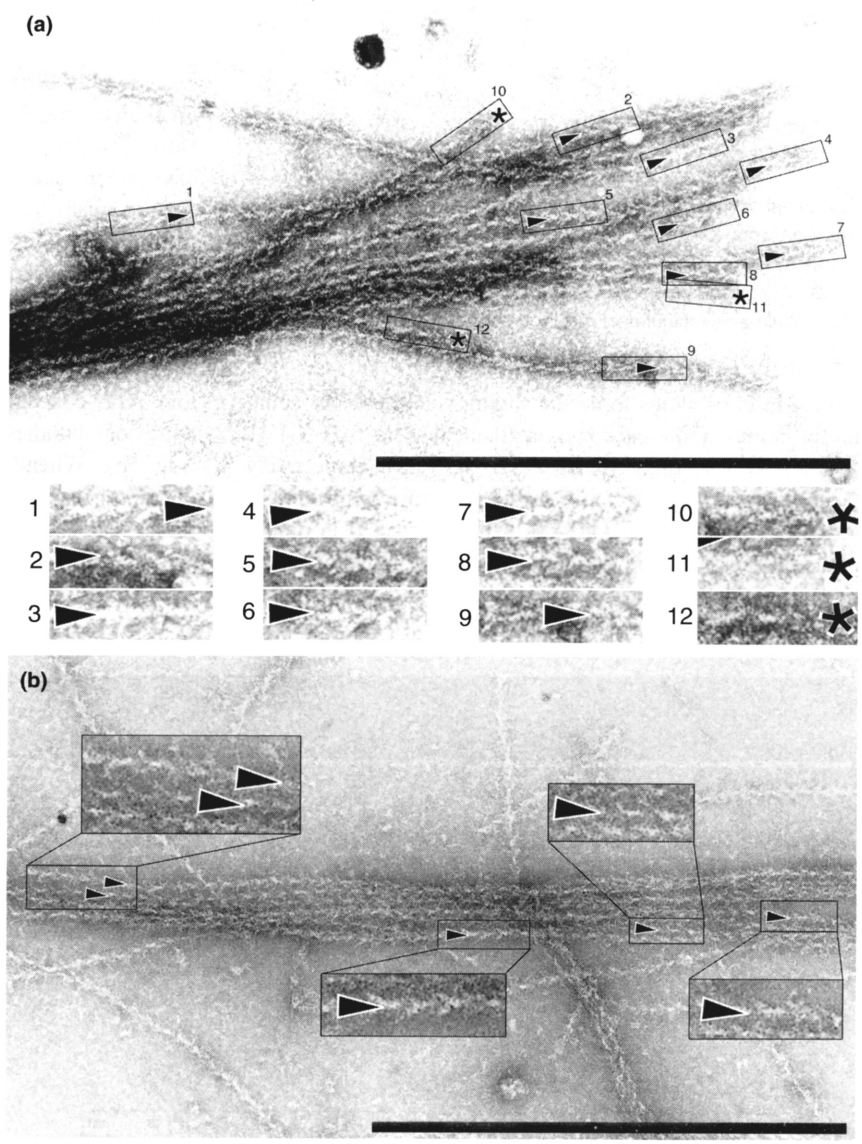

Fig. 2 Polarity of actin/fascin bundles. Electron micrographs of a negatively stained bundle decorated with skeletal muscle HMM. Arrowheads indicate the orientation of 'arrowhead structures' of decorated filaments. Asterisks indicate the filaments whose orientations were unclear. As far as we could determine the orientation, 'arrowhead structures' of F-actin in the bundle pointed to the same direction. (a, top panel) Bundles were formed by mixing G-actin with fascin-1 for 1 h, then decorating with HMM. Bar, 1 μm (a, bottom panels) Indicated areas in the top panel were enlarged to double. (b) Bundles were decorated with HMM within a few minutes after mixing F-actin with fascin-1. Bar, 1 μm. Inset, indicated areas were enlarged to double.

(Fig. 1), F-actin in the bundles must be less flexible than free F-actin, and the bundle not exhibit large change in the direction of movement.

The sliding velocities of actin/fascin bundles were comparable with those of single F-actin filaments on skeletal muscle myosin II. When coverslips were coated with myosin II at

Table 2 Orientation of F-actin in the actin/fascin bundle

	Filaments in the bundle (*n*)	Orientation of filaments determined (*n*)	Pointed in the same direction?[a]
Case A[b]			
Bundle 1	12	9	Yes
Bundle 2	14	8	Yes
Bundle 3	12	11	Yes
Bundle 4	10	8	Yes
Bundle 5	13	10	Yes
Bundle 6	10	6	Yes
Bundle 7	10	9	Yes
Case B[c]			
Bundle 8	5	5	Yes
Bundle 9	5	5	Yes
Bundle 10	7	5	Yes
Bundle 11	3	3	Yes
Bundle 12	4	3	Yes
Bundle 13	4	4	Yes
Bundle 14	6	4	Yes

[a]Examined among the filaments whose orientations were determined. [b]Bundles were formed by mixing G-actin with fascin-1 for 1 h, then decorated with HMM. Two replicate experiments (bundle 1–3 and bundle 4–7) have been performed. [c]Bundles were decorated with HMM within a few minutes of mixing F-actin with fascin-1.

0.6 μM in filamentous form, the sliding velocity of the actin/fascin bundle and single F-actin filament were 5.21 ± 1.11 and 5.53 ± 1.01 μm/s (mean ± SD, $n = 25$), respectively (Fig. 4a). At 0.1 μM myosin II, neither F-actin nor the bundles attached to the surface (Fig. 4a). When myosin II in monomeric form was applied to coverslips, the sliding velocities of bundles gradually decreased with a decreasing concentration of myosin II, showing a profile similar to that of single F-actin filaments (Fig. 4b). At 0.05 μM myosin II, neither filaments nor bundles attached to coverslips.

When ATP concentration in the assay buffer was varied, sliding velocity of single F-actin filament gradually decreased with decreasing ATP concentration (open circles). The sliding velocity of the actin/fascin bundle (closed circles) was the same as that of F-actin at every ATP concentration examined within an experimental error. The ATPase activities of myosin II (0.10 μM) activated by F-actin (4.2 μM) and by actin/fascin bundle (4.2 μM actin and 2.2 μM fascin) were 0.37 ± 0.04 and 0.34 ± 0.03/s (mean ± SD, $n = 5$), respectively. These results indicated that the modes of interaction of myosin II with actin/fascin bundles and with F-actin would be the same.

Disassembly of actin/fascin bundle during sliding on skeletal muscle myosin II

During sliding, actin/fascin bundles frequently disassembled when skeletal muscle myosin II concentration for coating was increased to 0.6 μM (Fig. 5a). Under the control conditions of 0.3 μM myosin II for coating, 84% of bundles slid farther than 20 μm without disassembly (Figs 3 and 5h). In contrast, when 0.6 μM myosin II was used for coating, 90% of bundles disassembled before sliding 15 μm. Similar disassembly was observed at the low ATP concentration of 20 μM in assay solution, and 84% of bundles disassembled within 10 μm sliding (Fig. 5h). When the bundle attached to the surface, the bundle became loose at the leading end and then 'unzipped' (Fig. 5a). In 85 out of 112 cases (76%), the leading end of the bundle was loosened and the rear end was packed (Fig. 5b–e). In other cases (24%), the bundle

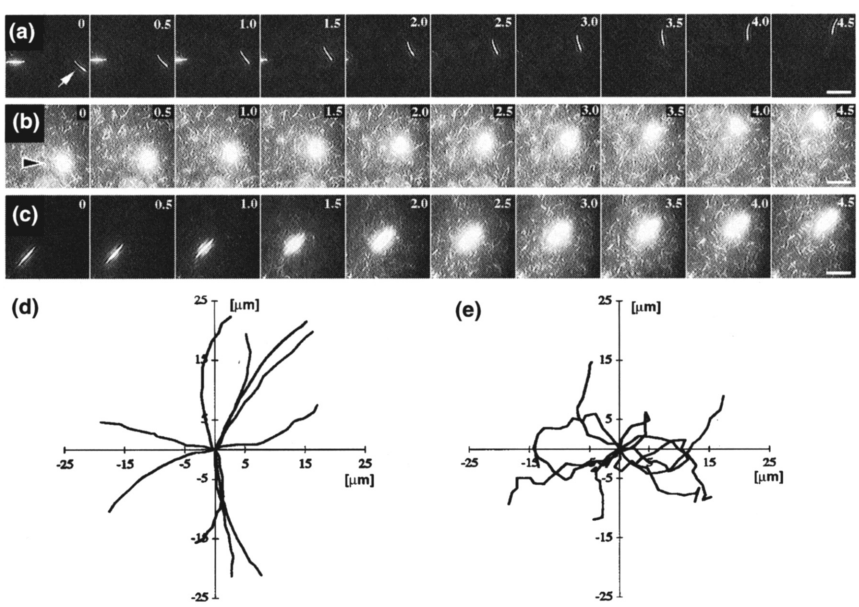

Fig. 3 Sliding movement of actin/fascin bundles on skeletal muscle myosin II. (a–c) Serial images of the bundle in the *in vitro* motility assay. The sensitivity of the camera was low (a), high (b), or was changed from low to high during observation (c). (d and e) Trajectories of the leading end of actin/fascin bundles (d) or F-actin without fascin (e) sliding on myosin II for 4 s. The positions at intervals of 0.25 s were plotted after alignment of the position at time zero to the origin of the axes. Actin filaments labelled with rhodamine-phalloidin were bundled with fascin, then applied to the assay chamber pre-coated with 0.3 μM myosin II. Numbers at the top right in each panel indicate time in seconds. Bars, 10 μm.

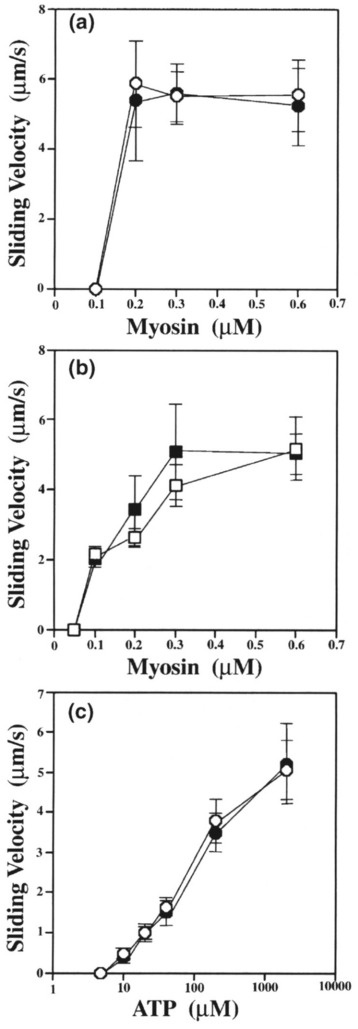

Fig. 4 Sliding velocities of actin/fascin bundles under various conditions. Skeletal muscle myosin II in filamentous form (a) or in monomeric form (b) at various concentrations was absorbed on coverslips. (c) ATP concentration in the assay buffer was varied. Open symbols indicate the sliding velocities of single F-actin filaments, and closed symbols indicate those of actin/fascin bundles. No filaments or bundles attached to the surface of coverslips coated by myosin II at 0.1 μM (a), and at 0.05 μM (b). At 5 μM ATP, both filaments and bundles attached to the surface of coverslips but did not slide. Sliding velocities of bundles ($n = 25$) at 0.6 μM myosin II in panels (a) and (b) were determined by monitoring the position of the rear ends at 25-s intervals for 1.5–4 s. For the rest of myosin concentrations, velocities of bundles or filaments ($n = 25$) were measured at intervals of 0.25 s for 4 s.

disassembled to filaments as soon as it attached to coverslips (Fig. 5f) or slid without disassembly. Because myosin II is a barbed-end-directed motor, the leading end of the actin/fascin bundle should be the pointed end. Thus, actin/fascin bundles disassembled from the pointed end. Images of dissociated filaments seemed to be as bright as single filaments in the background (Fig. 5a, panel 5.6). Actually, when we measured the brightness of images, filaments in the tips of dissociating bundles were as bright as the background filaments (Fig. 5i). Therefore, it seemed likely that actin/fascin bundles disassembled into single filaments.

The apparent dissociation constant of human fascin for F-actin is estimated to be 0.15–0.3 μM (Ono *et al.* 1997). Fascin concentration (0.02 μM) in our *in vitro* motility assay was about one-tenth of this value. However, when we changed microscopic focus to the middle of the assay chamber, floating actin/fascin bundles were seen without disassembly (Fig. 5g), and floating single filaments were not observed, except that single filaments were added in the assay buffer just before observation. It was also noted that bundles slid without disassembly on 0.3 μM myosin II (Figs 3 and 5h). These results suggested that disassembly was not due to dilution of actin/fascin bundles for the *in vitro* motility assay. We also examined whether attachment of myosin II to the glass surface of the assay chamber was necessary for disassembly of the bundles. As shown in Fig. 5(j and l), no disassembly of actin/fascin bundles was observed, even though they were incubated for 20 min with 0.6 μM myosin II in the presence of 2 mM ATP. When 0.3 μM myosin II was mixed with actin/fascin bundles in the presence of 20 μM ATP, the bundles showed no change in the first 2–3 min of incubation (data not shown). Five minutes after mixing, actin/fascin bundles gradually assembled (data not shown), and large aggregates of actin/fascin bundles were observed after 20 min incubation with myosin II (Figs 5k and m). This aggregation may be caused by rigor binding of myosin II to the actin/fascin bundles, because large aggregates of actin/fascin bundles were observed within 1 min after the mixture of myosin II in the absence of ATP (data not shown). These results suggested that disassembly of actin/fascin bundles was not due to the chemical process of myosin-binding to actin, but that it was caused by interaction with myosin on the surface.

Sliding and disassembly of actin/fascin bundles on non-muscle myosin II and myosin V

Next, we examined the sliding and disassembly of actin/fascin bundles on the surface coated with 0.12 μM non-muscle myosin. On this surface, actin/fascin bundles slid with an average velocity of 0.114 ± 0.021 μm/s (Figs 6a and e). Under the same conditions, single F-actin filaments slid at an average velocity of 0.109 ± 0.015 μm/s ($n = 25$) (Fig. 6e). Disassembly of the bundle was observed on non-muscle myosin II when concentration of myosin II used for coating was increased from 0.12 to 24 μM (Fig. 6b).

Myosin V localizes in filopodia of nerve growth cones (Wang *et al.* 1996). Therefore, we examined the sliding of actin/fascin bundles on chicken-brain myosin V. As shown in Figs 6(c and f), actin/fascin bundles slid on myosin V with an average velocity of 0.47 ± 0.10 μm/s. Under the same

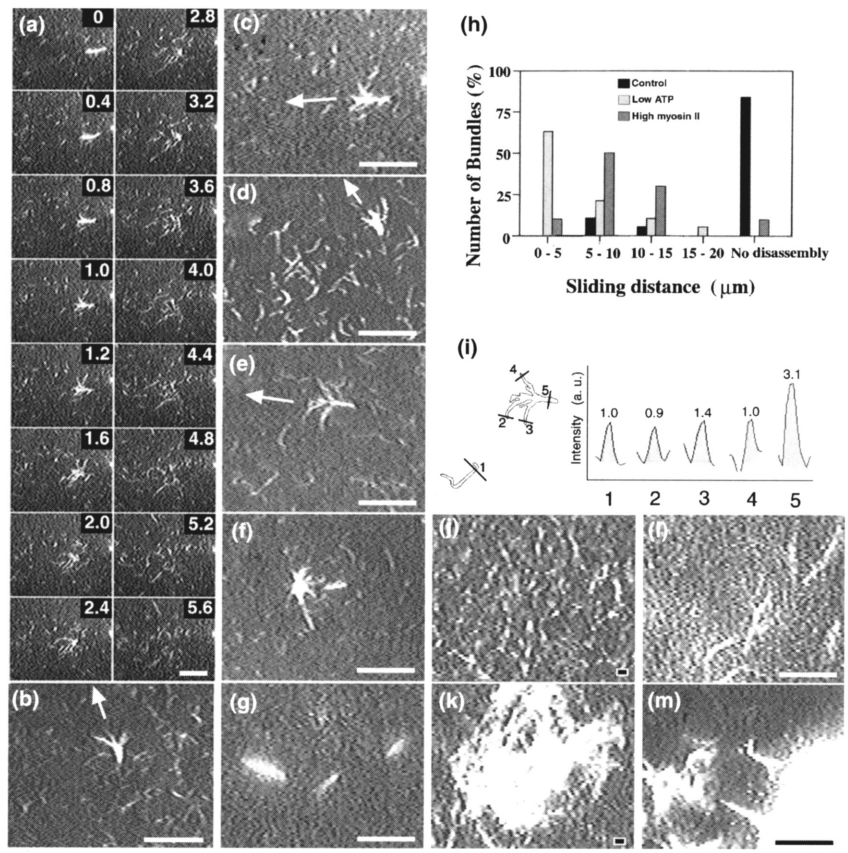

Fig. 5 Disassembly of actin/fascin bundles sliding on high density of skeletal muscle myosin II or at low concentration of ATP in the assay solution. (a) Serial images of the disassembling bundle sliding on myosin II absorbed at 0.6 μM in filamentous form. (b–f) Examples of partially loosened bundles during sliding. Arrows indicate the direction of movement of the bundle. (g) Actin/fascin bundles floating in assay solution. Focus was changed to the middle of the chamber after observation of disassembly and movement of bundles. (h) Histogram of the ratio of bundles disassembled within the indicated length of sliding. Control conditions, 0.3 μM myosin II for coverslip coating and 2 mM ATP in the assay solution; low ATP condition, 0.3 μM myosin II for coverslip coating and 20 μM ATP in the assay solution; high myosin II conditions, 0.6 μM myosin II for coverslip coating and 2 mM ATP in assay solution. Control and low ATP, $n = 19$; high myosin II, $n = 9$. (i, left) Trace of disassembling bundle and background F-actin presented in (e). F-actin labelled with rhodamine-phalloidin (2 nM) was simultaneously added to the assay solution, and one of the filaments with minimum brightness in the field was chosen as a background F-actin. (i, right) Pixel brightness of indicated cross-sections in left panel was quantified with NIH image software. The number at the top of each peak indicates the relative value of shaded area. (j–m) Without attaching to the surface of the assay chamber, myosin II did not cause the disassembly of actin/fascin bundles. Actin/fascin bundles were mixed in solution with 0.6 μM myosin II in the presence of 2 mM ATP (j and l), or 0.3 μM myosin II in the presence of 20 μM ATP (k and m), and observed 20 min after incubations. (j, k) Low magnifications; (l, m) high magnifications. Two replicated experiments were performed to confirm the results. Bars 10 μm.

conditions, single F-actin filaments slid at an average velocity of 0.56 ± 0.11 μm/s ($n = 25$). Disassembly of the bundle was also observed on myosin V when the concentration of myosin V used for coating was increased from 0.1 to 0.2 μM (Fig. 6d).

Discussion

Actin dynamics in filopodia is well organized. Actin is incorporated into the tips of filopodia, transported toward the basal region by 'retrograde flow', and then actin bundles disassemble to F-actin and/or depolymerize to G-actin in the basal region (Okabe and Hirokawa 1991; Lin *et al.* 1996; Katoh *et al.* 1999; Mallavarapu and Mitchison 1999). For these movements, the polarity of the actin bundle seems to be essential. If bundles were formed with random orientation of F-actin, G-actin could not be incorporated into the tips of filaments evenly, and bundles could not be transported unidirectionally by myosins. Indeed, intact bundles of actin filaments in filopodia have polarity (Lewis and Bridgman 1992). How are these polarized bundles of F-actin generated? Under the membrane of the lamellipodial tip, PIP2/cdc42/N-WASP complex coupled with Arp2/3 is suggested to enhance barbed end polymerization (Banzai *et al.* 2000; Rohatgi

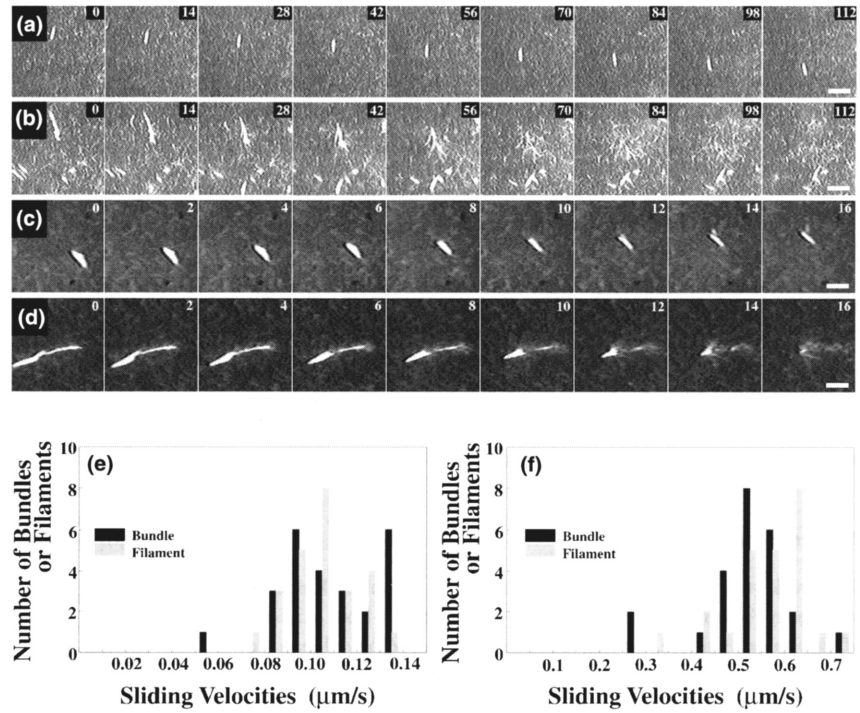

Fig. 6 Sliding and disassembly of actin/fascin bundles on non-muscle myosin II and myosin V. Non-muscle myosin II at 0.12 μM (a) or 0.24 μM (b), myosin V at 0.1 μM (c) or 0.2 μM (d) was absorbed to the surface. Assay conditions; non-muscle myosin II, 80 mM KCl, 5 mM $MgCl_2$, 2 mM ATP, 0.1 mM EGTA, and 20 mM MOPS (pH 7.2); myosin V, 75 mM KCl, 2 mM $MgCl_2$, 2 mM ATP, 1 mM EGTA, and 25 mM imidazole-Cl (pH 7.0). Two replicated experiments were performed to confirm the results. Bars, 10 μm. (e and f) Histograms of the sliding velocities of actin/fascin bundles (black bars) and actin filaments (grey bars) on non-muscle myosin II (e) and on myosin V (f). $n = 25$. Myosin concentrations used for coating were 0.12 μM in the case of non-muscle myosin II (e) and 0.10 μM in the case of myosin V (f).

et al. 2000), and form a dendritic network of F-actin with the barbed end pointing to lamellipodial tip (Svitkina and Borisy 1999). (Svitkina *et al.* 2003) recently showed that the actin bundle of filopodium splays apart at the root into individual F-actin filaments, and becomes an integral part of the lamellipodial network of F-actin in non-neuronal cells. They postulate that filopodial bundles arise by fusion of individual filaments in the dendritic network of lamellipodia. If this is the case, fascin may fasten loose actin filaments into a tight bundle as a zipper and form a polarized bundle. It is also possible that fascin may recruit F-actin to form polarized bundles by utilizing 'correct' directional F-actin as a seed. In both cases, our findings on the polarity of the actin/fascin bundle formed *in vitro* (Fig. 2, Table 2) strongly suggest that fascin plays an essential role in the formation of polarized bundles of F-actin in filopodia.

Myosins are suggested to be involved in growth-cone dynamics. Disruption of the actin–myosin interaction by microinjection of N-ethylmaleimide-treated S1, or by treatment with the myosin inhibitor 2,-3-butanedione monoxime stalls retrograde flow, resulting in elongation of the filopodia (Lin *et al.* 1996; Zhou and Cohan 2001). In contrast, knockout of myosin IIB, with its antisense oligonucleotide, inhibits neurite elongation in a differentiated neuroblastoma cell line (Wylie *et al.* 1998; Wylie and Chantler 2001). A similar result is obtained with cultured neurons from myosin IIB knockout mice (Bridgman *et al.* 2001). Furthermore, neurites elongate even in the absence of growth cones after treatment with cytochalasin in some neurons (Marsh and Letourneau 1984; Forscher and Smith 1988), although these results are still controversial (Neely and Gesemann 1994). The actomyosin system implicated in growth-cone dynamics and neurite elongation may be regulated through closely related but different signalling pathways, which cross talk with each other.

The distance between cross-linked actin filaments in filopodia is 7–8 nm (Lewis and Bridgman 1992). Purified human fascin also crosslinks F-actin with a distance of 8–9 nm (Figs 1a and b, Table 1). Therefore, it seems difficult for the myosin head to interact with F-actin inside the bundle. Our finding that actin/fascin bundles slide on myosin II and myosin V as fast as single F-actin filaments (Figs 4 and 6) suggests that retrograde flow is driven by direct interaction between myosins and F-actin filaments located in the surface of the filopodial bundle. The speed of retrograde flow is 0.02–0.12 μm/s depending on cell type (Okabe and Hirokawa 1991; Lin *et al.* 1996; Mallavarapu and Mitchison 1999). In our *in vitro* motility assay, actin/fascin bundles slide 0.1 μm/s on non-muscle myosin II (Fig. 6), 0.5 μm/s on myosin V (Fig. 6), and 5–6 μm/s on skeletal muscle myosin II (Fig. 4). Therefore, it seems likely that the type of myosin(s) involved in retrograde flow may affect the speed of retrograde flow, although we cannot directly compare the speed of retrograde flow *in vivo* with that *in vitro* because of no load in the *in vitro* motility assay. The type of myosin(s) involved in retrograde flow remains to be demonstrated.

Actin bundles disappear at the basal region of filopodia, which is suggested to be caused by bundle disassembly and/or depolymerization to G-actin (Katoh *et al.* 1999;

Mallavarapu and Mitchison 1999). Recently, the bundle of the basal region of filopodium is shown to splay apart, and becomes an integral part of the surrounding actin network of lamellipodium (Svitkina *et al.* 2003). Therefore, it seems likely that the disappearance of the actin bundle at the basal region of filopodia is caused by bundle disassembly, of which the driving force may be generated by myosin(s). If myosin concentration in the basal region of filopodia is high, filopodial bundles may disassemble into actin filaments in the same way as actin/fascin bundles disassemble in the *in vitro* motility assay (Fig. 5). Indeed, myosin II is reported to concentrate in the basal region of filopodia (Bridgman and Dailey 1989). Our findings may be a first step towards solving the molecular mechanism of dynamics in filopodia during path finding of axonal growth.

Acknowledgements

This work was supported by a Grant-in-Aid for Scientific Research on Priority Areas(C)-Advanced Brain Science Project-from Ministry of Education, Culture, Sports, Science and Technology, Japan (to RI), and a Grant from The Fujisawa Foundation (to RI).

References

Adelstein R. S. and Klee C. B. (1981) Purification and characterization of smooth muscle myosin light chain kinase. *J. Biol. Chem.* **256**, 7501–7509.

Ando T., Kodera N., Takai E., Maruyama D., Saito K. and Toda A. (2001) A high-speed atomic force microscope for studying biological macromolecules. *Proc. Natl Acad. Sci. USA* **98**, 12468–12472.

Banzai Y., Miki H., Yamaguchi H. and Takenawa T. (2000) Essential role of neural Wiskott–Aldrich syndrome protein in neurite extension in PC12 cells and rat hippocampal primary culture cells. *J. Biol. Chem.* **275**, 11987–11992.

Bentley D. and Toroian-Raymond A. (1986) Disoriented pathfinding by pioneer neuron growth cones deprived of filopodia by cytochalasin treatment. *Nature* **323**, 712–715.

Bridgman P. C. and Dailey M. E. (1989) The organization of myosin and actin in rapid frozen nerve growth cones. *J. Cell Biol.* **108**, 95–109.

Bridgman P. C., Dave S., Asnes C. F., Tullio A. N. and Adelstein R. S. (2001) Myosin IIB is required for growth cone motility. *J. Neurosci.* **21**, 6159–6169.

Bryan J. and Kane R. E. (1978) Separation and interaction of the major components of sea urchin actin gel. *J. Mol. Biol.* **125**, 207–224.

Bryan J., Edwards R., Matsudaira P., Otto J. and Wulfkuhle J. (1993) Fascin, an echinoid actin-bundling protein, is a homolog of the *Drosophila* singed gene product. *Proc. Natl Acad. Sci. USA* **90**, 9115–9119.

Cant K., Knowles B. A., Mooseker M. S. and Cooley L. (1994) *Drosophila* singed, a fascin homolog, is required for actin bundle formation during oogenesis and bristle extension. *J. Cell Biol.* **125**, 369–380.

Cheney R. E. (1998) Purification and assay of myosin V. *Meth. Enzymol.* **298**, 3–18.

Chien C.-B., Rosenthal D. E., Harris W. A. and Holt C. E. (1993) Navigational errors made by growth cone without filopodia in the embryonic *Xenopus* brain. *Neuron* **11**, 237–251.

Cohan C. S., Welnhofer E. A., Zhao L., Matsumura F. and Yamashiro S. (2001) Role of the actin bundling protein fascin in growth cone morphogenesis: localization in filopodia and lamellipodia. *Cell Motil. Cytoskeleton* **48**, 109–120.

DeRosier D. J. and Censullo R. (1981) Structure of F-actin needles from extract of sea urchin oocytes. *J. Mol. Biol.* **146**, 77–99.

Edwards R. A. and Bryan J. (1995) Fascin, a family of actin bundling proteins. *Cell Motil. Cytoskeleton* **32**, 1–9.

Edwards R. A., Herrera-Sosa H., Otto J. and Bryan J. (1995) Cloning and expression of murine fascin homolog from mouse brain. *J. Biol. Chem.* **270**, 10764–10770.

Forscher P. and Smith S. J. (1988) Action of cytochalasins on the organization of actin filaments and microtubules in a neuronal growth cone. *J. Cell Biol.* **107**, 1505–1516.

Hong K., Nishiyama M., Henley J., Tessier-Lavigne M. and Poo M.-M. (2000) Calcium signaling in the guidance of nerve growth by netrin-1. *Nature* **403**, 93–98.

Ishikawa R., Yamashiro S., Kohama K. and Matsumura F. (1998) Regulation of actin binding and actin bundling activities of fascin by caldesmon coupled with tropomyosin. *J. Biol. Chem.* **273**, 26991–26997.

Kane R. E. (1975) Preparation and purification of polymerized actin from sea urchin egg extracts. *J. Cell Biol.* **66**, 305–315.

Katoh K., Hammer K., Smith P. J. S. and Oldenbourg R. (1999) Birefringence imaging directly reveals architectural dynamics of filamentous actin in living growth cones. *Mol. Biol. Cell* **10**, 197–210.

Kodama T., Fukui K. and Kometani K. (1986) The initial phosphate burst in ATP hydrolysis by myosin and subfragment-1 as studied by a modified malachite green method for determination of inorganic phosphate. *J. Biochem. (Tokyo)* **99**, 1465–1472.

Kureishy N., Sapountzi V., Prag S., Anilkumar N. and Adams J. C. (2002) Fascins, and their roles in cell structure and function. *Bioessays* **24**, 350–361.

Lau P.-M., Zucker R. S. and Bentley D. (1999) Induction of filopodia by direct local elevation of intracellular calcium ion concentration. *J. Cell Biol.* **145**, 1265–1275.

Lewis A. K. and Bridgman P. C. (1992) Nerve growth cone lamellipodia contain two populations of actin filaments that differ in organization and polarity. *J. Cell Biol.* **119**, 1219–1243.

Lin C. H., Espreafico E. M., Mooseker M. S. and Forscher P. (1996) Myosin drives retrograde F-actin flow in neuronal growth cones. *Neuron* **16**, 769–782.

Mallavarapu A. and Mitchison T. (1999) Regulated actin cytoskeleton assembly at filopodium tips controls their extension and retraction. *J. Cell Biol.* **146**, 1097–1106.

Marsh L. and Letourneau P. C. (1984) Growth of neurites without filopodial or lamellipodial activity in the presence of cytochalasin B. *J. Cell Biol.* **99**, 2041–2047.

Matsumura F., Yamashiro-Matsumura S. and Lin J. J.-C. (1982) Isolation and characterization of tropomyosin-containing microfilaments from cultured cells. *J. Biol. Chem.* **258**, 6636–6644.

Neely M. D. and Gesemann M. (1994) Disruption of microfilaments in growth cones following depolarization and calcium influx. *J. Neurosci.* **14**, 7511–7520.

Okabe S. and Hirokawa N. (1991) Actin dynamics in growth cone. *J. Neurosci.* **11**, 1918–1929.

Ono S., Yamakita Y., Yamashiro S., Matsudaira P. T., Gnara J. R., Obinata T. and Matsumura F. (1997) Identification of an actin binding region and a protein kinase C phosphorylation site on human fascin. *J. Biol. Chem.* **272**, 2527–2533.

Otto J. J. (1994) Actin-bundling proteins. *Curr. Opin. Cell Biol.* **6**, 105–109.

Otto J. J., Kane R. E. and Bryan J. (1979) Formation of filopodia in coelomocytes: localization of fascin, a 58,000 dalton actin cross-linking protein. *Cell* **17**, 285–293.

Pato M. D., Sellers J. R., Preston Y. A., Harvey E. V. and Adelstein R. S. (1996) Baculovirus expression of chicken nonmuscle heavy meromyosin II-B. *J. Biol. Chem.* **271**, 2689–2695.

Perry S. V. (1955) Myosin adenosintriphosphatase. *Meth. Enzymol.* **2**, 582–588.

Rohatgi R., Ho H. Y. and Kirschner M. W. (2000) Mechanism of N-WASP activation by CDC42 and phosphatidylinositol 4,5-biphosphate. *J. Cell Biol.* **150**, 117–120.

Sakamoto T., Amitani I., Yokota E. and Ando T. (2000) Direct observation of processive movement by individual myosin V molecules. *Biochem. Biophys. Res. Commun.* **272**, 586–590.

Sasaki Y., Hayashi K., Shirao T., Ishikawa R. and Kohama K. (1996) Inhibition by drebrin of the actin-bundling activity of brain fascin, a protein localized in filopodia of growth cones. *J. Neurochem.* **66**, 980–988.

Steketee M. B. and Tosney K. W. (2002) Three functionally distinct adhesions in filopodia: shaft adhesions control lamellar extension. *J. Neurosci.* **22**, 8071–8083.

Steketee M., Balazovich K. and Tosney K. W. (2001) Filopodial initiation and a novel filament-organizing center, the focal ring. *Mol. Biol. Cell* **12**, 2378–2395.

Svitkina T. M. and Borisy G. G. (1999) Arp2/3 complex and actin depolymerizing factor/cofilin in dendritic organization and treadmilling of actin filament array in lamellipodia. *J. Cell Biol.* **145**, 1009–1026.

Svitkina T. M., Bulanova E. A., Chaga O. Y., Vignjevic D. M., Kojima S., Vasiliev J. M. and Borisy G. G. (2003) Mechanism of filopodia initiation by reorganization of a dendritic network. *J. Cell Biol.* **160**, 409–421.

Tilney L. G., Tilney M. S. and Guild G. M. (1995) F actin bundles in *Drosophila* bristles. I. Two filament cross-links are involved in bundling. *J. Cell Biol.* **130**, 629–638.

Toyoshima Y., Kron S. J., McNally E. M., Niebling K. R., Toyoshima C. and Spudich J. A. (1987) Myosin subfragment-1 is sufficient to move actin filaments *in vitro*. *Nature* **328**, 536–539.

Tseng Y., Fedorov E., McCaffery J. M., Almo S. C. and Wirtz D. (2001) Micromechnics and ultrastructure of actin filament networks crosslinked by human fascin: a comparison with α-actinin. *J. Mol. Biol.* **310**, 351–366.

Wang F.-S., Wolenski J. S., Cheney R. E., Mooseker M. S. and Jay D. G. (1996) Function of myosin-V in filopodial extension of neuronal growth cones. *Science* **273**, 660–663.

Wylie S. R. and Chantler P. D. (2001) Separate but linked functions of conventional myosins modulate adhesion and neurite outgrowth. *Nat. Cell Biol.* **3**, 88–92.

Wylie S. R., Wu F.-J., Patel H. and Chantler P. D. (1998) A conventional myosin motor drives neurite outgrowth. *Proc. Natl Acad. Sci. USA* **95**, 12967–12972.

Yamashiro-Matsumura S. and Matsumura F. (1985) Purification and characterization of an F-actin-bundling 55-kilodalton protein from HeLa cells. *J. Biol. Chem.* **260**, 5087–5097.

Zheng J. Q. (2000) Turning of nerve growth cones induced by localized increases in intracellular calcium ions. *Nature* **403**, 89–93.

Zheng J. Q., Felder M., Connor J. A. and Poo M.-M. (1994) Turning of nerve growth cones induced by neurotransmitters. *Nature* **368**, 140–144.

Zhou F. Q. and Cohan C. S. (2001) Growth cone collapse through coincident loss of actin bundles and leading edge actin without actin depolymerization. *J. Cell Biol.* **153**, 1071–1084.

